Persistence Length and Molecular Mass Distribution of a Thermotropic Main-Chain Liquid-Crystal Polymer

Herbert Krömer,* Rainer Kuhn,* Harald Pielartzik, and Wilfried Siebke

Bayer AG, Zentrale Forschung, D-5090 Leverkusen, FRG

Volker Eckhardt

Bayer AG, Geschäftsbereich Kunststoffe, D-4150 Uerdingen, FRG

Manfred Schmidt

Max-Planck-Institut für Polymerforschung, D-6500 Mainz, FRG

Received June 9, 1990; Revised Manuscript Received September 15, 1990

ABSTRACT: 3,5-Bis(trifluoromethyl)phenol (BTFMP) is found to be a good solvent for many fully aromatic thermotropic liquid-crystalline (LC) copolyesters, which are useful as high-temperature resistent thermoplastics. A typical random copolyester, composed of 70 mol % *p*-hydroxybenzoic acid and 30 mol % 2-hydroxy-6-naphthoic acid units, was fractionated from BTFMP solution with Decalin as the precipitant. The original polymer sample and the fractions were studied in detail by viscometry, integrated light scattering (ILS), photon correlation spectroscopy (PCS), and size-exclusion chromatography (SEC). The molar mass distributions were determined by SEC measurements, calibrated by the viscometry and ILS data of the fractions. From the molecular dimensions obtained by ILS and PCS, the persistence length was determined to (12.0 ± 1.0) nm in BTFMP at 60 °C. This means that in dilute solution the polymer molecules do not resemble perfectly rigid rods, but are rather comparable to typical semiflexible chains consisting of approximately 2–20 persistence lengths. The molecular dimensions were also determined in solvent mixtures with decreased solvating power. The coil size remained constant, although the second virial coefficient decreased, but still remained positive. These effects are attributed to the stiffness of the chains.

Introduction

Thermotropic main-chain liquid-crystal polymers are advanced new materials of considerable commercial interest since they offer a unique combination of properties such as high thermal and chemical resistance, high stiffness, low melt viscosity, and good processing behavior. Linear aromatic polyesters form the most important class of thermotropic LC polymers that have been developed and commercialized so far. Aromatic polyesters consisting of perfectly linear chain molecules like poly(*p*-hydroxybenzoic acid) (poly-HBA) undergo thermal degradation before reaching the melting point and cannot be processed in the molten state. Comonomers that disturb the translational symmetry of the chain do not fit into the ideal crystal lattice of poly-HBA and will hence reduce the crystallinity and the melting point so that the copolymer can be processed by injection molding, extrusion, etc. The molten polymer may form an anisotropic LC phase if the chains contain sufficiently long straight sequences that are able to align in a parallel arrangement. The rheological properties and the processing behavior of the LC phase depend on the stiffness and average curvature of the chains. Reliable analytical methods for the determination of the molar mass distribution and of the curvature of the molecules are therefore essential for the optimization of the structure and properties of LC polymers.

A new solvent, 3,5-bis(trifluoromethyl)phenol, is now available that allows the molecular characterization of most thermotropic LC copolyesters in dilute solution.[1] Several aromatic LC polymers differing in their chemical composition were studied in this way. In this paper we report the results for one particular LC polymer.

Experimental Section

Polymer Composition. The investigated polymer was a fully aromatic copolyester consisting of 70 mol % *p*-hydroxybenzoic acid (HBA) units and 30 mol % 2-hydroxy-6-naphthoic acid (HNA) units. The chains are expected to be completely linear since no branching, e.g., trifunctional, monomers were used in the synthesis. The polymer was not exposed to high temperatures, which might have induced branching, cross-linking, or degradation reactions. The distribution of HBA and HNA units along the chains is random according to X-ray diffraction measurements of HBA(70)/HNA(30) copolymers[2-4] that had been synthesized under similar conditions. The molten polymer exhibited typical liquid-crystalline properties, e.g., a birefringent domain morphology.

Viscometry. The apparent viscosity number was measured in dilute 3,5-bis(trifluoromethyl)phenol solution at 60 °C by using a modified Ubbelohde viscometer with a coiled capillary (for reducing the shear stress and hence avoiding non-Newtonian behavior of the polymer). The limiting viscosity number $[\eta]$ was obtained by extrapolating the data to zero concentration in a Huggins or Arrhenius plot.

Fractionation. LC polymer (5 g) was dissolved in 600 mL of BTFMP at room temperature. The polymer was then fractionated at constant temperature (90 °C) by precipitation, with Decalin at 90 °C as precipitating agent. The polymer concentration at the precipitation of the first fraction was 3.3 g/L. The coacervates of the fractions obtained in this way were dissolved in BTFMP and reprecipitated with cyclohexane at 45 °C in order to facilitate the removal of solvent.

Size Exclusion Chromatography. SEC measurements were carried out at 60 °C with a high-temperature chromatograph (Millipore Waters, Model 150 C) and BTFMP as the eluent. Since polystyrene is soluble in BTFMP as well ($[\eta] = 2.78 \times 10^{-4} M^{0.63}$ at 60 °C; $[\eta]$, dL/g; M, g/mol), the SEC measurements of the LC polymer and the fractions of this product were performed with a series of four commercial PS-Lichrogel columns (PS 40 000/PS 4000/PS 400/PS 40; Merck, Darmstadt, Germany). Dilute solutions (ca. 1 g/L) were purified by filtration through disposable PTFE filters of 0.45-μm pore size (Millipore Waters). The elution rate was 0.6 cm³/min (injected sample volume 100 μL). A high-temperature differential refractometer

0024-9297/91/2224-1950$02.50/0

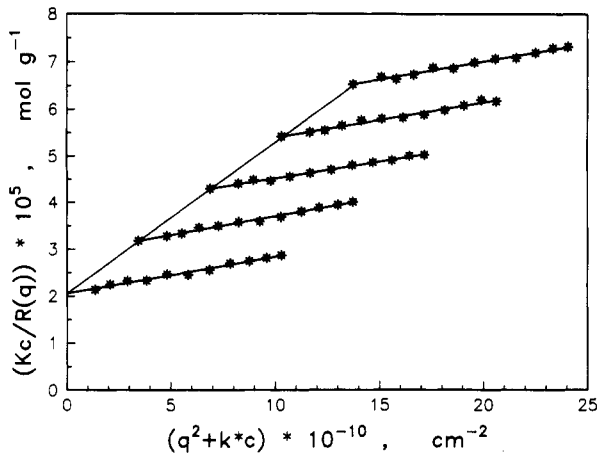

Figure 1. Zimm plot of integrated light scattering data for fraction 1 (Kc/R, mol/g, as function of $q^2 + kc$, cm^{-2}; BTFMP, 60 °C; concentrations c = 0.97, 1.95, 2.92, and 3.90 g/L).

served for determining the relative polymer concentration during the elution process. The "universal" SEC calibration curve was established by plotting $[\eta]M_w$ vs the elution volume, utilizing the measured intrinsic viscosities and the molecular weights obtained by light scattering.

Although the LC polymer is soluble in BTFMP at room temperature, all measurements were carried out at 60 °C for two purposes: First, for reducing the viscosity of the solvent and hence also the axial dispersion, and second, for avoiding the crystallization of BTFMP at the high pressure within the SEC columns (the crystallization point of BTFMP is 20 °C, the boiling point 176 °C).

Light Scattering. Measurements: Integrated and dynamic light scattering was measured with a commercial instrument consisting of a ALV/SP-85 goniometer and ALV-3000 correlator developed by Schätzel,[5] which is suitable for simultaneous static and dynamic light-scattering measurements (photon correlation spectroscopy). The commercially available software as developed by Eisele[6] controls the angular-dependent measurements and performs the data acquisition and evaluation as described below.

Light-scattering measurements were carried out in BTFMP (60 °C) at concentrations of 1–5 g/L. Vertically polarized 514.5-nm radiation of an argon ion laser served as the light source. An interference filter was employed in order to minimize the contribution of fluorescence to the scattering intensity. Several measurements were performed at each scattering angle (between 30 and 150 °C). Thus, poor measurements caused by dust or microgel particles could be identified and discarded. Sampling times for photon counting were set at sufficiently small values, typcially in the order of 1–5 μs, so that the initial decay of the correlation function could be precisely determined.

Toluene at 60 °C was employed as secondary standard (R = 3.411×10^{-5} cm^{-1} at $\theta = 90°$) for the determination of the absolute scattering intensities. The refractive index increment dn/dc was determined by means of a Brice-Phoenix instrument to be 0.236 ± 0.002 cm^3/g for the original LC polymer as well as for all the fractions. The viscosity of the solvent, 2.25 mPa s at 60 °C, was measured with a capillary viscometer.

Evaluation: The integrated light-scattering intensities were evaluated according to Zimm's method by plotting Kc/R vs $q^2 + kc$ where

$$K = (4\pi^2 n_s^2/N_A\lambda_0^4)(dn/dc)^2 \qquad q = 4\pi n_s \sin(\theta/2)/\lambda_0 \qquad (1)$$

and c = concentration, R = excess scattering of the solution in cm^{-1} = "Rayleigh's ratio", k = arbitrary constant, n_s = refractive index of the solvent, N_A = Avogadro's number, λ_0 = vacuum wavelength, θ = scattering angle. From the Zimm plot (see, e.g., Figure 1) the weight-average molar mass M_w, the z-average mean-squared radius of gyration, R_g^2, and the second virial coefficient A_2 were determined in the usual way (n_s = 1.3991 for 514.5-nm radiation at 60 °C).

In dynamic light scattering, the time correlation function of the scattering intensity $g_2(t)$ is measured, which usually is converted to the electric field correlation function $g_1(t)$ via the Siegert relation:

$$g_1(t) = [(g_2(t) - A)/A]^{1/2} \qquad (2)$$

with A the experimentally determined base line. The correlation function $g_1(t)$ was analyzed according to the method of cumulants.[7]

$$\ln g_1(t) = -\Gamma t + (1/2!)\mu_2\Gamma^2 t^2 - (1/3!)\mu_3\Gamma^3 t^3 + \ldots \qquad (3)$$

With $\Gamma = -(d \ln g_1(t)/dt)_{t\to 0}$. Γ is called the first cumulant; μ_2 and μ_3 measure the deviation from a single-exponential decay. To all correlation functions a second- or third-order cumulant fit was applied. Extrapolated to zero angle, the reduced first cumulant Γ/q^2 yields the apparent diffusion coefficient D_{app}.

The z-average diffusion coefficient D_z is obtained by extrapolating D_{app} to $c \to 0$ and $q^2 \to 0$, e.g., by means of a "dynamic Zimm plot".[8] The hydrodynamic radius R_h is then calculated from D_z by the Stokes equation:

$$R_h \equiv \langle 1/R_h \rangle_z^{-1} = kT/6\pi\eta_0 D_z \qquad (4)$$

where k = Boltzmann's constant, and η_0 = 2.25 mPa s = viscosity of the solvent at 60 °C.

Results

Fractionation and Properties of Fractions. Table I summarizes experimental results of the original polymer sample and of the fractions obtained by successive fractional precipitation. The fractionation gave somewhat inconsistent results, e.g., quite different weight percentages of the fractions. These irregularities may be due to crystallization by cooling during the decantation of the solution from the precipitate. However, the subsequent characterization unambiguously demonstrated that the fractionation procedure yielded samples sufficiently narrow for further investigations.

Figure 2 displays a plot of log $[\eta]$ vs log M_w. From the data for the fractions the following relationship was obtained ($[\eta]$ in dL/g, M_w in g/mol):

$$[\eta] = 9.93 \times 10^{-4} M_w^{0.842} \qquad (5)$$

This relation certainly represents only an approximation, because in the present range of chain stiffness it is theoretically well-known that the log $[\eta]$ vs log M_w plot is slightly curved. This slight curvature is not observed experimentally because of the rather narrow investigated molecular weight range and the limited accuracy of the experimental data.

The point corresponding to the unfractionated polymer lies very close to the interpolated line for the fractions in Figure 2; this is expected because the exponent a = 0.842 is rather close to a = 1. (For a = 1, the influence of the polydispersity on $[\eta]$ and on M_w is exactly the same, which means that the above relationship holds also for fairly wide M_w distributions with M_w/M_n up to 3.) The light-scattering measurements were in some cases slightly disturbed by dust, especially at scattering angles below 50°. Sometimes a small number of dust particles could not be removed completely by filtration. (Ultracentrifugation was ineffective since these particles had densities like that of the solvent, 1.465 at 60 °C.) However, the static LS measurements could be reliably extrapolated down to $q^2 = 0$. Repeated measurements on LC polymers in BTFMP gave the following approximate values for the precision of integrated light scattering results: M_w: ±4%; A_2 ±10%; R_g: ±5% (at least 1 nm).

Dynamic light scattering showed no dependence of the apparent diffusion coefficient $D_{app}(c)$ on q^2 within experimental error. The z-average diffusion coefficient D_z was obtained by extrapolation of $D_{app}(c)$ to $c = 0$. The precision

Table I
Distribution of Polymer Structure and Dimensions (BTFMP, 60 °C)

					struct data from light scattering					struct data from SEC			
sample	precipitant added,[a] mL	wt fraction, %	100 − $J(M)$, %	$[\eta]$, dL/g	M_w, g/mol	10^3A_2, mol cm^3 g^{-2}	R_g, nm	R_h, nm	$\rho = R_g/R_h$	$M_{n,calc}$, g/mol	$M_{w,calc}$, g/mol	$(M_w/M_n)_{calc}$	$[\eta]_{calc}$, dL/g
orig polym fraction		100		7.1	36 000	7.2	32	11.5	2.8	13 800	43 900	3.18	7.40
1	900	9.8	4.9	6.4	36 000	7.8	33	13	2.5	20 200	46 000	2.28	7.77
2	910	71.7	45.7	6.1	31 000	7.8	29	11	2.6	16 300	30 900	1.90	5.69
3	950	2.7	82.9	8.0	43 000	8.6	38	13	2.9	19 300	40 900	2.11	7.19
4	1050	1.5	85.0	5.2	25 000	6.9	22	10	2.2	18 800	26 000	1.39	5.08
5	1300	8.2	89.8	2.9	13 000	7.0	13	6	2.2	11 100	14 000	1.26	3.03
6	2000	6.1	96.9	1.78	7 500	6.4		4.5		6 100	8 000	1.30	1.89

[a] Decalin.

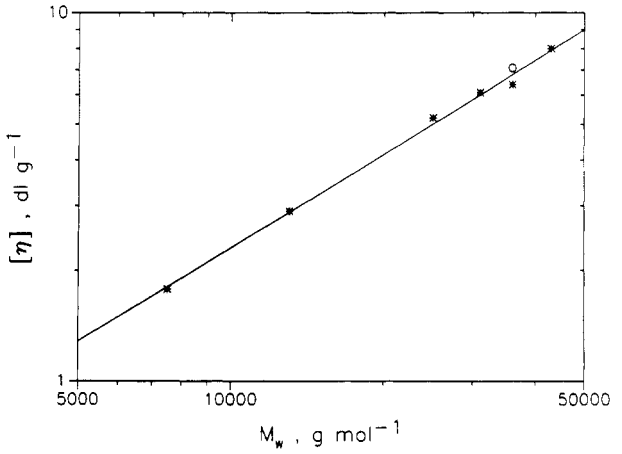

Figure 2. Limiting viscosity number $[\eta]$ as a function of molecular mass M_w (BTFMP, 60 °C; * fractions, O original polymer; data point of original polymer not used in the interpolated solid line).

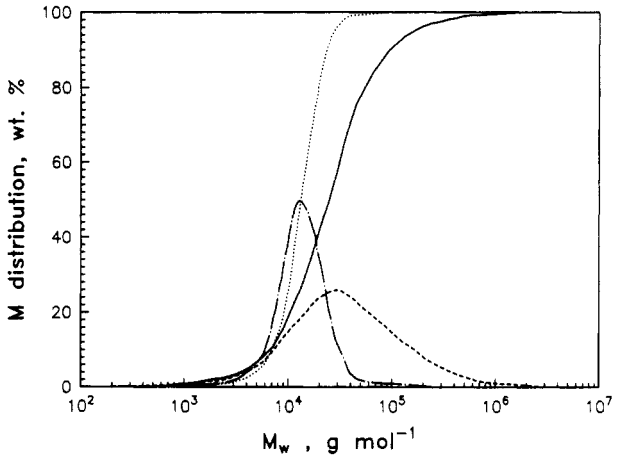

Figure 3. Differential and cumulative molecular mass distributions from SEC measurements (BTFMP, 60 °C) Original polymer: cumulative distribution (—); differential distribution (- - -). Fraction 5: cumulative distribution (· · ·); differential distribution (- · -).

of D_z values and hence of the hydrodynamic radius R_h is estimated to be ±4%.

Molar Mass Distribution. SEC elution curves were evaluated by employing a universal calibration curve $M[\eta]$ derived from eq 5 and corrected for axial dispersion. Figure 3 shows the fairly wide molar mass distribution of the original polymer sample and the much narrower distribution curve of one of the fractions. M_w and M_n values calculated from the SEC distribution curves and the polydispersity indices M_w/M_n are included in Table I. The M_w/M_n values vary between 3.2 for the unfractionated polymer and about 1.3 for the low molar mass fractions 5 and 6. This ratio increases, as usual, with increasing molar mass of the fractions.

Persistence Length. The persistence length l_p was obtained by numerical computation from the molar mass distribution and from R_g and R_h values of the fractions (Table I), based on the Kratky–Porod wormlike chain model.[9] The details of this procedure are briefly explained in the Appendix. The following parameters necessary for the computation were derived from the known composition of the polymer: M_0 = 135 g/mol average molecular mass per monomer unit; l_0 = 0.686 nm average contour length per monomer unit; d = 0.6 nm effective hydrodynamic cross section of the chain

Table II show the R_g and R_h values calculated by using the above parameters. It is seen that the best fit to the experimental data is obtained for the persistence length l_p = 12.0 nm. Figure 4 demonstrates the agreement between the experimental and the calculated data.

Polymer Dimensions in Different Solvents. Table III shows results of viscometric and light-scattering measurements on dilute solutions of the polymer in mixtures of BTFMP containing 0.0, 9.1, and 13.0 vol % of the nonsolvent *n*-butanol, which is nearly isorefractive with BTFMP. The polymer becomes insoluble in a mixture containing 16.7 vol % *n*-butanol (first cloud point). The second virial coefficient A_2 decreases slightly with increasing *n*-butanol concentration, but $[\eta]$, M_w, and R_g remain almost constant. The coefficient k_H of the Huggins equation

$$\eta_{sp}/c = [\eta] + k_H[\eta]^2c \qquad (6)$$

varies with the nonsolvent concentration of the mixed solvent as expected for a flexible polymer (η_{sp} = specific viscosity).

Discussion

Fractionation and Molar Mass Distribution. Repeated viscosity measurements showed that the limiting viscosity number of a dilute BTFMP solution of the LC polymer kept for several days at 80 °C remained constant within experimental error. This was verified by light-scattering measurements. Hence, it is assumed that the fractionation carried out at 90 °C did not lead to any substantial changes in the molar mass distribution. Since a satisfactory $[\eta]$–M_w relationship was obtained, SEC measurements could be reliably calibrated. For the highest molecular weight samples there are some discrepancies between the absolute molar masses determined by light scattering and the M_w values calculated from SEC elution curves (Table I). These inconsistent results are probably due to the limited validity of the universal calibration relationship at high molecular weights.

Table II
Determination of Persistence Length l_p (BTFMP, 60 °C)

	exptl results				theoretical results					
					l_p = 11.0 nm		l_p = 12.0 nm		l_p = 13.0 nm	
fraction	$L_{w,exp}$, nm	$R_{g,exp}$, nm	$R_{h,exp}$, nm	$((M_w/M_n) - 1)_{exp}$	$((M_w/M_n) - 1)_{th} = 1/m$	$R_{g,th}$, nm	$R_{h,th}$, nm	$R_{g,th}$, nm	$R_{h,th}$, nm	$R_{g,th}$, nm	$R_{h,th}$, nm
1	183	33	13	1.28	1	30.0	12.4	31.2	12.6	32.2	12.8
2	157.5	29	11	0.90	1	27.6	11.2	28.6	11.3	29.6	11.5
3	218.5	38	13.3	1.11	1	33.0	13.9	34.4	14.2	35.6	14.4
4	127	22	10	0.39	1/2	22.8	9.5	23.6	9.65	24.4	9.75
					1/3	21.9	9.45	22.7	9.6	23.4	9.7
5	66	13	6	0.26	1/4	14.3	5.95	14.6	6.0	15.0	6.5
6	38		4.5	0.30	1/3	10.0	4.02	10.3	4.14	10.5	4.06

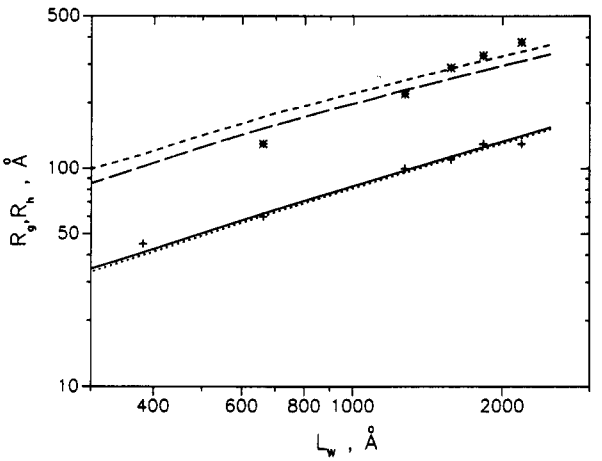

Figure 4. Radius of gyration R_g and hydrodynamic radius R_h as functions of molecular mass M_w (measured in BTFMP at 60 °C; theoretical curves computed with the persistence length l_p = 12.0 nm and Schulz–Zimm parameters m = 1 and 3): (*) $R_{g,exp}$; (+) $R_{h,exp}$; (- - -) $R_{g,th}(m=1)$; (—) $R_{h,th}(m=1)$; (– – –) $R_{g,th}(m=3)$, (· · ·) $R_{h,th}(m=3)$.

Persistence Length. Information on the conformation of polymer molecules in dilute solution can be obtained from the dependence of $[\eta]$, R_g, and R_h on the molar mass M_w (Figures 2 and 4). The approximate exponents of the $[\eta]$–M_w relationship, 0.84, and of the R_g–M_w relationship, 0.89, have similar values and are rather high. These exponents and the relatively high limiting viscosities and molecular radii indicate that the molecules are much more extended than conventional flexible polymers. The same conclusion follows from the high values of $\rho = R_g/R_h$, which lie between 2.9 and 2.2 (Table I); because of the increasing polydispersity ρ increases slightly with increasing molar mass. (For typical flexible chains an upper value $\rho \approx 1.7$ would be expected.) The quantitative determination of the chain stiffness based on the wormlike chain model yields a persistence length l_p = 12.0 nm. The error in l_p is estimated to be about ±10%; it is primarily due to the uncertainty of the radius of gyration of low molecular mass fractions. We believe that the described light-scattering investigation represents an excellent method for the determination of the persistence length of semiflexible chains. A special advantage of this method is to account explicitly for the polydispersity of polymers with rather wide molar mass distribution. Other scattering methods, such as small-angle X-ray and neutron scattering, may be less suitable for investigating polymers with broad molar mass distributions because the usually applied Kratky plot[10] often does not show a clearly recognizable plateau, so that the crossover point between the ascending branch of the scattering curve and the plateau cannot be accurately determined. The persistence length reported here compares qualitatively well with recent molecular dynamics simulations of Jung and Schürman,[11] who determined the persistence length of poly(*p*-hydroxybenzoic acid) to be l_p = 6.5 nm.

Influence of Solvent on Molecular Dimensions. The high second virial coefficients A_2 of the unfractionated polymer and of all the fractions (between 6.4×10^{-3} and 8.6×10^{-3} mol cm^3 g^{-2}) show that BTFMP is a good solvent for this material at 60 °C (and at 25 °C as well). The A_2 values of the fractions are slightly different but do not vary systematically with the molecular weight. (Normally A_2 decreases with increasing molecular mass but is independent of molecular mass for rods.) The different A_2 values of the fractions are probably mainly due to experimental error.

The polymer properties measured in binary solvent mixtures of BTFMP and *n*-butanol show some unusual features (Table III). For example, $[\eta]$ and M_w remain nearly constant when the solvent composition is changed from 0 to 13.0 vol % *n*-butanol, although the polymer is insoluble in a mixture containing 16.7 vol % *n*-butanol. This means that no association occurs even in solvent compositions quite close to the precipitation point. The second virial coefficient A_2 decreases when the *n*-butanol percentage is increased, but remains unusually high even for the solvent containing 13 vol % butanol. R_g is nearly independent of the solvent composition. We attribute this behavior to the stiffness of the chains, but we cannot offer a satisfactory explanation. Thermodynamically the probably predominant entropic portion of A_2 originates from the total excluded volume of the dissolved polymer. In the limiting case of stiff rods the intramolecular excluded volume vanishes since no contacts are possible between different sites of a rigid linear rod. The following simple formula hold for cylindrical rods (see, e.g., Elias[12]):

$$A_2 = v_{2,sp}{}^2/2\pi r_{cyl}{}^3 N_A \qquad (7)$$

where $v_{2,sp}$ is the specific volume and r_{cyl} the radius of the rod. According to this formula, A_2 should not depend on chain length. This is in fact observed within the limits of experimental error (Table I). With $v_{2,sp}$ = 0.731 cm^3/g (solid polymer at 60 °C) and the effective hydrodynamic radius r_{cyl} = 0.3 nm (used for calculating the persistence length) one obtains $A_2 = 5.2 \times 10^{-3}$ mol cm^3 g^{-2}, which is not very different from the experimental value, $A_2 = 7.2 \times 10^{-3}$. This agreement is better than could be expected in view of the simplifications involved in the derivation of formula 7, but it surprisingly demonstrates that thermodynamically the polymer molecules interact almost like rigid rods. Apparently the number of intramolecular contacts within the polymer is very small, so that A_2 mainly depends on the external excluded volume of the solute. The unusually high value of A_2 in the vicinity of the precipitation point may probably be attributed to the stiffness of the chains. Since stiff molecules do not shrink when the quality of the solvent is reduced, the entropic

Table III
Polymer Properties in Solvent Mixtures of Different Solvating Power (60 °C)

n-butanol solvt,[a] vol %	[η], dL/g	k_H	dn/dc, cm³/g	M_w, g/mol	R_g, nm	R_h, nm	$\rho = R_g/R_h$	10^3A_2, mol cm³ g⁻²
0	7.1	0.36	0.236	36 000	32	11.5	2.8	7.2
9.1	7.0	0.51	0.251	38 000	35	14.0	2.5	6.0
13.0	7.25	0.57	0.257	38 000	36	14.2	2.5	5.5
16.7	insoluble							

[a] Main component: 3,5-bis(trifluoromethyl)phenol.

intermolecular interactions are not changed significantly, so that the entropic part of A_2 will likewise retain a high value up to the precipitation point. Phase separation at 60 °C occurs probably not by spinodal demixing, but by formation of an ordered crystalline or mesomorphic phase.

Acknowledgment. We express our gratitude to C. Beer, J. Sarnecki, J. Schwellenbach, and H. G. Würtz for carrying out the experiments.

Appendix

The evaluation of the persistence lengths from the molecular dimensions takes into account the polydispersity of the samples. For all samples a Schulz–Zimm distribution function of the molecular weight is assumed a priori, the convolution parameter m of which is adjusted to the experimentally determined M_w/M_n values:

$$W(L) = (L^m/m!)y^{m+1}\exp(-yL)$$

where $y = (m + 1)/L_w$ and L_w the weight average contour length of the polymer. The z-average mean-square radius of gyration

$$\langle s^2\rangle_z = \int_0^\infty w(L)L\langle s^2\rangle\, dL / \int_0^\infty w(L)L\, dL$$

was evaluated analytically for the radius of gyration of a Kratky–Porod wormlike chain according to Benoit and Doty[13] as[14,15]

$$(\langle s^2\rangle_z = (m + 2)l_k/6y - l_k^2/4 + yl_k^3/(m + 1)4 - (l_k^4/(8m(m + 1))(y^2 - y^{m+2}/(y + 2l_k)^m)$$

with l_k = Kuhn's statistical segment length = $2l_p$. According to eq 4 the hydrodynamic radius is measured as an inverse z-average:

$$\langle 1/R_h\rangle_z^{-1} = [\int_0^\infty w(L)LR_h^{-1}\, dL / \int_0^\infty w(L)L\, dL]^{-1}$$

The evaluation of the hydrodynamic radius of a Kratky–Porod wormlike chain is much more elaborate.[16] For the present purpose we applied the Koyama formulation[17] of the segment distribution function, which leads to a numerically soluble integral expression for the hydrodynamic radius.[18] It should be noted that the evaluation of the quantity $\langle 1/R_h\rangle_z^{-1}$ requires a double numerical integration,[15] for details of which the reader is referred to the original literature.

References and Notes

(1) Bayer AG; Inv. Kuhn, R.; Marhold, A.; Dicke, H. German Patent 3712817, 1989; U.S. Patent 4960539, 1990.
(2) Blackwell, J.; Gutierrez, G. A.; Chivers, R. A. *Macromolecules* **1984**, *17*, 1219.
(3) Biswas, A.; Blackwell, J. *Macromolecules* **1988**, *21*, 3146, 3152, 3158.
(4) Blackwell, J., private communication, 1990.
(5) Schätzel, K. *Opt. Acta* **1983**, *30*, 155.
(6) Eisele, M. Dissertation, Freiburg, 1988.
(7) Koppel, D. E. *J. Chem. Phys.* **1972**, *57*, 4814.
(8) Bantle, S.; Schmidt, M.; Burchard, W. *Macromolecules* **1982**, *15*, 1604.
(9) Kratky, O.; Porod, G. *Recl. Trav. Chim. Pays-Bas* **1949**, *68*, 1106.
(10) Kratky, O. *Pure Appl. Chem.* **1966**, *12*, 483.
(11) Jung, B.; Schürmann, B. L. *Macromolecules* **1989**, *22*, 477.
(12) Elias, H. G. *Makromoleküle*, 2nd ed.; Hüthig & Wepf Verlag: Basel, 1972; p 199.
(13) Benoit, H.; Doty, P. *J. Phys. Chem.* **1953**, *57*, 958.
(14) Oberthür, R. C. *Makromol. Chem.* **1978**, *179*, 2693.
(15) Schmidt, M. *Macromolecules* **1984**, *17*, 553.
(16) Yamakawa, H.; Fujii, M. *Macromolecules* **1974**, *7*, 649.
(17) Koyama, R. *J. Phys. Soc. Jpn.* **1973**, *34*, 1029.
(18) Schmidt, M.; Stockmayer, W. H. *Macromolecules* **1984**, *17*, 509.